ADVANCED FUNCTIONAL MATERIALS
www.afm-journal.de

Epoxide Speciation and Functional Group Distribution in Graphene Oxide Paper-Like Materials

*Adrian Hunt, Dmitriy A. Dikin, Ernst Z. Kurmaev, Teak D. Boyko, Paul Bazylewski, Gap Soo Chang, and Alexander Moewes**

The electronic structure and chemical bonding of three differently prepared samples of graphene oxide paper-like sheets are studied. Two are created by water filtration of fully oxidized graphene sheets, although one is later intercalated with dodecylamine. The third is created by reducing graphene oxide with hydrazine hydrate. The spectroscopic fingerprints of the aligned epoxide functional groups that unzip the carbon basal plane are found. This unzipping appears to be a result of aging, and the extent to which the basal plane is unzipped can be controlled via the preparation method. In particular, reduction with hydrazine enhances line defect formation, whereas intercalation inhibits the process.The hydroxyl functional group also has a tendency to gather in zones of dense oxidation on the carbon basal plane, a predilection that is not shared by the other prominent functional group species. Finally, the non-functionalized carbon sites exhibit very similar bonding despite the increase in the sp^2/sp^3 ratio, confirming that reduction alone is insufficient for producing pristine graphene from graphene oxide. These results are obtained by directly probing the electronic structure of the graphene oxide samples via X-ray absorption near-edge structure spectroscopy (XANES) and resonant X-ray emission spectroscopy (RXES). This work has important significance for the development of graphene oxide as a band gap-engineered electronic material, as preparation methodology strongly affects not only the initial condition of the sample, but how the electronic structure evolves over time.

1. Introduction

Graphene has attracted much interest of late as the first two-dimensional crystal ever experimentally realized.[1] Pristine graphene is a zero-band gap semiconductor with electrons behaving like massless Dirac fermions,[2] although doped graphene will stray from this simple but elegant band structure.[3] Graphene is a material that has been suggested for use in supercapacitors,[4] as a hydrogen storage medium,[5–7] and even in integrated circuits as active components as well as interconnects.[8] If graphene were used as an interconnect, the ballistic transport properties alone would make it an excellent choice.[9] Organic photovoltaic researchers have also looked at graphene for use as an intermediate layer between two cells.[10] However, the question of how to most efficiently synthesize graphene remains. One option is to first make graphene oxide by exfoliating graphite oxide in water or another polar solvent[11] then reduce the harvested graphene oxide sheets to make graphene.[12] This process is easily scalable to industrial production levels, and thus is a more cost-effective manufacturing method than the micro-mechanical exfoliation method used to first isolate graphene.

Beyond its use as a graphene precursor material, however, graphene oxide may prove to be a useful material in its own right. Graphene oxide, because of its solubility in common solvents, has been used to replace both the typical indium tin oxide (ITO) electrode[13,14] and the equally ubiquitous soluble fullerene-derivative n-type organic semiconductor, PCBM, in organic solar cells,[15,16] and has also been shown to function as a photocatalyst.[17] Chemically-reduced graphene oxide has also been suggested as a detector for airborne molecules.[18] Perhaps one of the most ambitious suggestions for the use of graphene oxide is to employ this material in electronic devices, replacing silicon in integrated circuits. However, the lack of a noticeable band gap in graphene limits its utility for electronics applications. It is therefore important to develop methods to induce and control a band gap in graphene. A band gap may be created in graphene using one of two methods: by functionalizing graphene[19] or by chemically treating graphene oxide.[20] With the natural tendency of graphene oxide to stack in ordered layers, and with pristine graphene functioning as highly conductive and chemically stable interconnects, a new era of carbon- based electronics may be realized.[21] However, many problems must be overcome before these goals may be realized, not the least of which being able to properly and reproducibly

A. Hunt, T. D. Boyko, P. Bazylewski, Prof. G. S. Chang, Prof. A. Moewes
Department of Physics and Engineering Physics
University of Saskatchewan,116 Science Pl
Saskatoon, Saskatchewan, S7N 5E2, Canada
E-mail: alex.moewes@usask.ca
Prof. D. A. Dikin
Department of Mechanical Engineering
Northwestern University
2145 Sheridan Road, Evanston, IL, 60208-3111, USA
Dr. E. Z. Kurmaev
X-ray Emission Spectroscopy Lab
Institute of Metal Physics
RAS Ural Div., 18 Kovalevskoi Str., Yekaterinburg 620990, Russia

DOI: 10.1002/adfm.201200529

control the electronic and physical structure of graphene oxide. Many have theorized about the structure of graphene oxide and its precursor graphite oxide,[22–26] and there have been many experimental studies using various techniques to characterize these materials.[27–30] In particular, X-ray absorption near-edge fine structure (XANES) studies of graphite oxide have been highly useful in elucidating the local electronic structure of the carbon and oxygen sites in graphene oxide.[31–35]

Despite the impressive work done on graphene oxide, many questions persist as to the structure of this material. One particularly poignant question concerns the bond integrity of the carbon lattice under the strain of functional group bonding. The functional groups, originally attached to the 2D carbon plane to make graphene oxide soluble, may serve to alter the electronic and physical structure of graphene in a variety of beneficial or deleterious ways. The epoxide functional group has attracted special focus because some studies have suggested that this functional group may serve to unzip the C-C intraplanar bonds in graphene.[24] Line defects have been visually observed in HOPG,[36] and unzipping carbon nanotubes to produce graphene nanoribbons is a very active area of research.[37] To answer some of these questions, we present an experimental comparison of three samples of graphene oxide paper, all prepared in different ways. These samples were studied using synchrotron-based X-ray absorption near-edge fine structure (XANES) and resonant X-ray emission spectroscopy (RXES), so that the oxygen and carbon states could be probed separately for detailed, element- and site-specific information.

2. Results and Discussion

Graphene research in general, and graphene oxide research in particular, has proceeded quickly down many different paths as researchers attempt to find the optimal ways to make, and use, these materials, This study focuses on three of the archetypal graphene oxide products: "fully" oxidized graphene oxide (GOp), graphene oxide paper that has been reduced with hydrazine hydrate (rGOp),[12] and graphene oxide paper that has been intercalated with dodecylamine (iGOp). All three samples were made into paper-like products using a methodology described elsewhere.[38,39] **Table 1** below details the overall C:O ratio for each of the three samples, as well as the approximate C:O ratio for each functional group. Oxygen in water was not included in the C:O ratios.

Table 1. C:O ratios for all three samples at the time of synthesis. The overall ratio includes only the oxygen contained within functional groups bonded to the carbon basal plane and does not account for any intercalated water.

Sample system	Overall ratio C(graphene):O	Ratios for oxygen-containing groups		
		Epoxide	Hydroxyl	Carbonyl/Carboxyl
GOp	2.9	4.9	19.3	11.15
rGOp	5.0	16.7	9.8	26.3
iGOp	2.6	5.8	18.6	6.3

To confirm and expand upon our understanding of the chemical structure of the three samples of graphene oxide paper, let us turn to angular-resolved XANES spectra of the three samples, measured while exciting upon the C 1*s*–2*p* resonant absorption threshold. As mentioned earlier, aside from C 1*s* XPS, C 1*s* XANES experiments have thus far been the most prevalent method of characterizing graphene and graphene oxide systems using X-rays. **Figure 1** presents the C 1*s* XANES spectra. Generally speaking, the spectra show many of the features that one expects to find in graphene oxide as

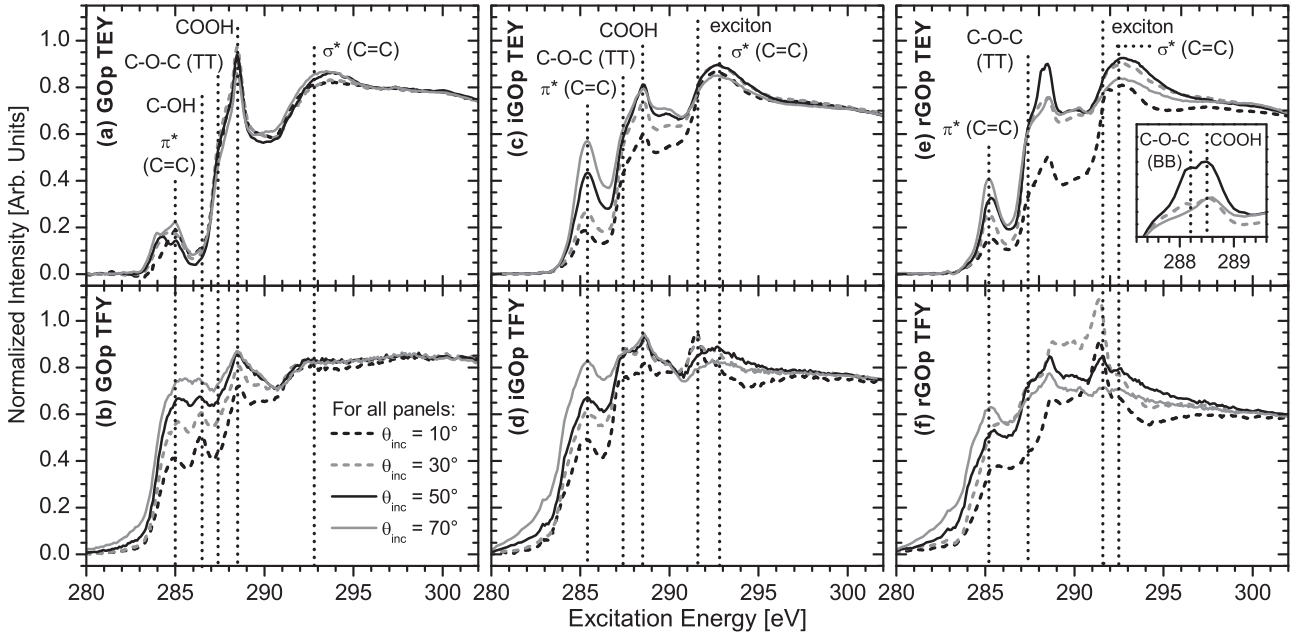

Figure 1. Angular-resolved XANES spectra, measured simultaneously in total electron yield (TEY) and total fluorescence (TFY) modes while the incident radiation was 30 from the surface normals of the samples. All of the spectra in a particular panel have been normalized to a common point at high energy. a) TEY of GOp. b) TFY of GOp, measured simultaneously with the TEY. c) TEY of iGOp. d) TFY of iGOp. e) TEY of rGOp, with an inset zooming into the 288.5 eV resonance features. f) TFY of rGOp.

found in previous studies,[31–35] which are labeled according the anti-bond that is being resonantly filled at that energy. These features are generally attributed to different functional groups by comparison of the C 1*s* XANES spectra of graphene oxide to spectra of simpler systems with similar structure. As an example, consider benzoic acid, phthalic acid, pyrocatechol, and salicylic acid, which are compounds with carboxyl and/or hydroxyl functional groups attached to a benzene ring. The C 1*s* XANES spectra of these compounds clearly show a peak structure that changes according to the relative mix of hydroxyl and carboxyl bonding.[40] This allows one to assign the peaks seen in the C 1*s* XANES spectra of graphene oxide to the functional groups that gave rise to them in the spectra of the benzene-based acids.

There is, however, one marked difference between our spectra and those that have been published by others. The inset in Figure 1e shows a zoomed view of the rGOp spectra, focused on the region around 288.5 eV. It is quite clear that two features are resolved: one at 288.2 eV, and one at 288.5 eV. The 288.5 eV is a common and prominent feature in other reported XANES studies of graphene oxide and graphite oxide, but the 288.2 eV feature, to the best of our knowledge, has not previously been seen. It is not present, or at least not resolved, in the TEY spectra of either of the other two samples at any angle.

As we shall later show, this 288.2 eV feature is the spectral signature of a particular allotrope of epoxide that can occur if the normals of the surface defined by the C-O-C triangle of many epoxide groups align collinearly. This alignment makes spontaneous breaking of the C=C bond energetically favorable, forming a defect line,[24,41] although the mechanism powering the break is in dispute.[36,42] This so-called unzipping of the carbon basal plane can break graphene into pieces, possibly to the benefit of nanotechnological applications if controlled properly.[43] This type of epoxide we call broken bond epoxide (BB-epoxide). Although we shall show that the 288.2 eV feature is due to BB-epoxide, there is insufficient evidence at this point in the analysis to reach that conclusion. Given that the 288.2 eV feature is most prominent in rGOp, it could be due to a product of the reduction process, a functional species that was always present and has a higher resistance to hydrazine than other functional groups, or it is an aging effect.

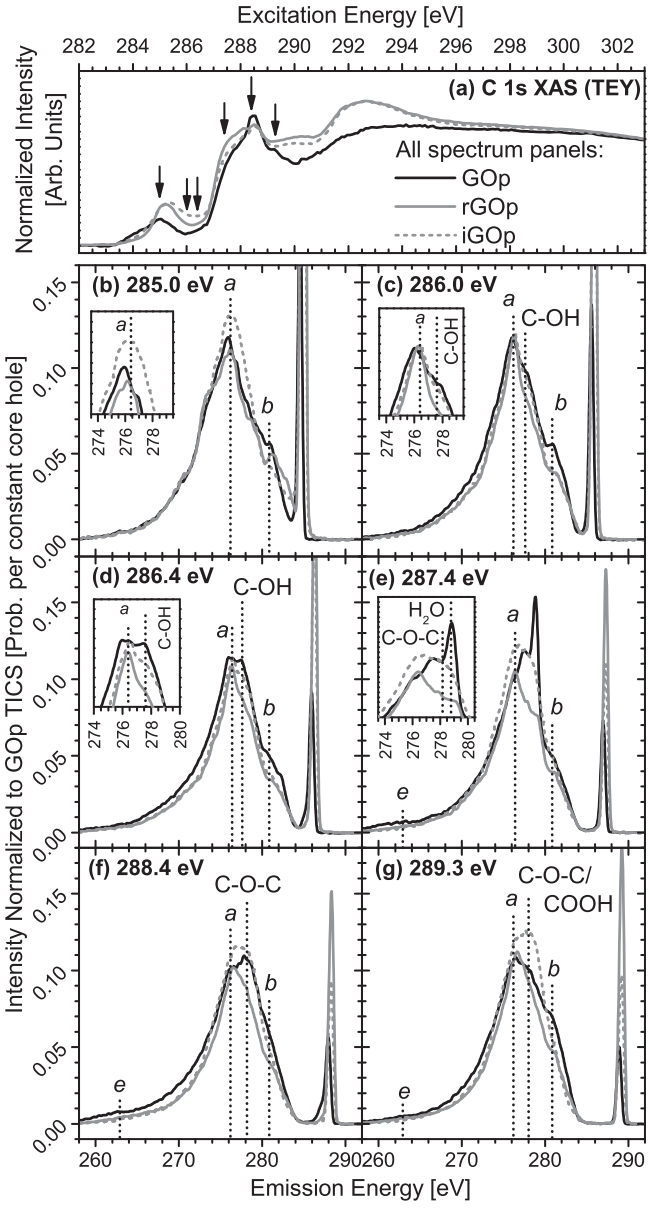

Figure 2. C Kα RXES spectra of graphene oxide paper. a) XANES spectra of the three samples to indicate graphically where the excitation energies are on the threshold. b–g) RXES spectra of GOp, rGOp, and iGOp measured while exciting each sample the energy indicated in the bold title block in the top left corner of each panel. All spectra had background counts subtracted and were smoothed with an 10-point FFT filter and normalized to calculated GOp TICS. Insets in (b–e) show a zoomed window of the spectra where differences are easier to see. Several prominent features are labeled with the functional group that is the most probable main contributor to the bulk of the measured spectral weight.

2.1. Functional Group Dispersion and Ordering

More details are clearly needed in terms of the bonding, particularly concerning this newly observed functional group. Let us therefore turn to RXES. This technique allows one to resonantly excite the different functional groups and probe the local bonding environment that each sees. RXES spectra were measured while exciting the three differently-prepared samples of graphene oxide paper listed earlier at six distinct energies that include the approximate binding energies of the functional groups observed in Figure 1. **Figure 2** shows the results of the RXES experiment.

Intuitively, the differences among the lineshapes of the three samples should indicate differences among the bonding environments seen by the sites probed by the incident X-rays. The question then becomes how one can appropriately normalize the spectra from the samples under scrutiny so that peak intensity differences are physically meaningful. The method chosen for this study is normalization by total integrated counts per second (TICS) ratio. A description of the calculation of experimental TICS is detailed in the Experimental Section. In short, normalizing spectra by a common TICS value allows quantitative comparison of peak intensities among spectra of different

Table 2. Literature C 1*s* XPS binding energies of functional groups in graphitic and graphenic systems.

C-ring π^*	Hydroxyl C−O	Epoxide C−O−C	Carbonyl C=O	Carboxyl COOH	Carbonate CO_3	Ref.
	286.7	287.2		288.2		[49]
285.0	286.4	287.2		289.4		[35]
284.9 - 285.1	286.3 - 286.9	287.2 - 287.8		289.0 - 289.6		[50]
284.6 - 285.1	286.3 - 287.0		287.5 - 288.1	289.3 - 290.0		[51]
284.1	286.7	288.3			290.0	[52]
284.8	286.2		287.8	289.0		[53]
284.5	286.5				290.5	[54]
284.6	286.1		287.5	289.2		[55]
284.6	286.6		288.5			[56]
284.3	286.1		287.4	288.1		[57]

compounds by compensating for differences among the core hole creation rates of the samples. The ratio of TICS values between two samples gives the relative core hole creation rate.

The effect that each functional group has on the electronic structure is different, particularly when considering the optical properties that are so important to the application of graphene oxide to organic photovoltaic research.[44] Thus, the distribution of the functional groups and any remaining non-functionalized carbon becomes a key concern. This issue is particularly relevant to the reduction process because the different functional groups do not react with various reducing agents (in this case, hydrazine) to the same degree. The degree of homogeneity in functional group dispersion will thus directly impact the structure of the end product. Lerf and Klinowski[27,28] have proposed that graphene oxide does not oxidize uniformly based upon ^{13}C NMR studies of graphite oxide. This idea has been supported by later studies on graphite oxide[45] and on graphene oxide,[46,47] although it does contradict other proposed models.[48]

Our results show that the Lerf-Klinowski non-uniform oxidation pattern holds, but with a further refinement. We show that dense oxidation zones contain most of the bonded hydroxyl groups, whereas epoxides and carboxyls are more evenly dispersed. Uncovering the evidence for this conclusion begins, perhaps paradoxically, with the study of the non-functionalized carbon sites, hereafter called pristine graphene-like (PG-like) states. The local bonding pDOS of these sites are detailed in the RXES spectra shown in Figure 2b, measured while exciting the samples at 285.0 eV. This excitation energy is very close to the main π^* resonance in HOPG at 285.4 eV, but below the resonant excitation energies for the major functional groups (see **Table 2**). As one can see in Figure 2b, the iGOp spectrum shows a higher a/b peak height ratio than either GOp or rGOp. The reason for this will be touched upon later, but for now, let us focus on the fact that peak *a* in iGOp is characteristically higher than that in the spectra of either GOp or rGOp, The intensity variation pattern of peak *a* in the 285.0 eV spectra is also seen in Figure 2e–g, However, this pattern is not seen in Figure 2c or d. The consensus among authors using XPS is that a photon with an energy that falls in the range of 286.0 eV to 286.4 eV will resonantly excite a C atom bound to a hydroxyl functional group.[35,49–57] These XPS results are summarized in Table 2. It would seem that, when exciting a hydroxyl group, the PG-like states do not fluoresce nearly as strongly. It is clear that the hydroxyl functional groups electronically interact poorly with PG-like states. This suggests that hydroxyl groups bunch together in zones of dense oxidation, separated physically and electronically from zones of light oxidation where PG-like states occur. The other functional groups do not seem to experience this separation, resonant excitation of epoxide (287.2–288.3 eV) and carboxyl (288.5 eV) shows the return of PG-like fluorescence.

The reason for the higher a/b peak height ratio in the 285.0 eV spectrum of iGOp is that intercalating dodecylamine between the graphene oxide planes produced a more ordered sample. In structures similar to graphite, peak *a* is due to emission from in-plane σ-symmetry bonds, and *b* is due to out-of-plane bonding, The out-of-plane bonding can either be σ-symmetry in sp^3 bonding, or π-symmetry in sp^2 bonding; at 285.0 eV, any sp^2 bonding present will be resonantly excited. Analogous to XANES spectra, a higher contrast between the σ and π emission lines means greater ordering. Thus, we can conclude that iGOp is a graphene oxide derivative that has more ordered planar structure. As we shall show later in the paper, this is because the carbon planes in iGOp have not been unzipped by suitably aligned epoxide functional groups.

Returning to Figure 2b, one is struck by how similar are the spectra of GOp and rGOp. This shows that the PG-like states are qualitatively very similar in the two compounds. The significance of this observation is that, while chemical reduction does increase the sp^2/sp^3 ratio and thus increases the number of non-functionalized carbon atoms, reduction does not make the bound carbon states more graphene-like. The likely reason for this is that distortions to the carbon basal plane from oxidation remain after reduction.

Within Figure 2, characteristic emission lines from the different functional groups were highlighted. The assignment of a spectral feature in a C Kα spectrum to emission from a particular functional group was done simply by looking at which functional group was being resonantly excited at the excitation energy in question. For example, in reference to Figure 1, the resonant excitation energy needed to create core holes on carbon sites bonded to hydroxyl (the C-OH bond) is about 286.4 eV. It is therefore logical that the emission line seen at 277.6 eV is due to the C-OH bond, For excitation energies 287.4 eV and 288.4 eV, the epoxide functional groups were resonantly excited. At these energies, the 277.6 eV feature seen previously was replaced by a feature at 278.2 eV due to emission from epoxide.

2.2. Epoxide Speciation

The C Kα spectra of Figure 2 have shown some important aspects of the bonding in graphene oxide, but the spectra measured while exciting at 288.4 eV show no discernible, characteristic emission line from the new functional group first detected

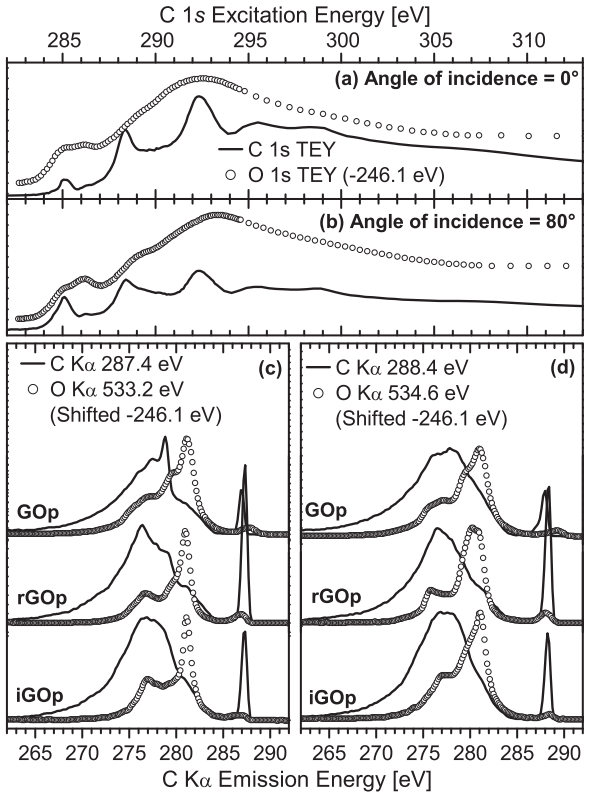

Figure 3. Threshold alignment of C and O states. High-resolution C 1*s* and O 1*s* XANES measured on GOp at a) 0° and b) 80°. Each O 1*s* XANES spectrum was shifted down in energy by 246.1 eV to line it up with its counterpart C 1*s* XANES spectrum. In (c), the O Kα spectra measured at 533.2 eV were shifted by –246.1 eV to compare to the C Kα spectra measured at 287.4 eV for all three samples (GOp, rGOp, and iGOp). Similarly, in (d), the O Kα spectra measured at 534.6 eV were shifted by –246.1 eV to compare to the C Kα spectra measured at 288.3 eV. Visual inspection shows that there are many peaks common between the two edges, which is what one would expect from strongly hybridized states shared by the oxygen and carbon sites.

at 288.2 eV excitation energy in the XANES spectra of rGOp. The reason for this is likely a combination of the large number of carbon states contributing to the 288.4 eV spectra and the large lifetime broadening inherent to many carbon systems. Both of these problems are effectively mitigated by turning to O Kα RXES spectroscopy to probe the functional groups separately. This will be particularly effective for differentiating BB-epoxide and its more commonly understood cousin, total triangle epoxide (TT-epoxide), the two allotropes of epoxide of interest here.

Before the O Kα RXES experiment can be used to probe the different epoxide allotropes, however, the proper excitation energies are needed. The resonant excitation energy for TT- epoxide is 287.4 eV, and we suspect the resonant excitation energy of BB-epoxide to be 288.2 eV on the C 1*s* threshold. Equivalent resonant excitation energies on the O 1*s* threshold were determined by shifting the O 1*s* XANES spectrum of GOp by –246.1 eV so that it matched, peak for peak, its C 1*s* XANES spectrum as shown in **Figure 3**a and b, under the constraint that the relative spacing between peaks lined up in this fashion would remain constant on both edges. The justification for this approach is that, regardless of the element one is resonantly exciting, one is promoting core electrons into the same hybridized anti-bonding states that are shared when C and O atoms bond. The idea that the unoccupied states should align should also apply to the occupied states, because the valence C pDOS and O pDOS are also heavily hybridized. The comparisons between the C Kα and O Kα spectra (shifted down by 246.1 eV like the O 1*s* XANES spectra) of the three samples are shown in the bottom six panels of Figure 3. The excellent alignment of the elastic peaks and some prominent inelastic features shows how well the 246.1 eV shift brings the two edges together.

Applying the 246.1 eV shift to the C 1*s* resonant excitation energies of 287.4 eV and 288.2 eV needed to resonantly excite the TT-epoxide and BB-epoxide groups, one should excite at approximately 533.5 eV and 534.3 eV, respectively. In reality, after careful calibration of the data post-experiment, the samples were excited at 533.2 eV and 534.6 eV. The influence of carboxyl and water were qualified using spectra taken from published liquid cell experiments of acetic acid[58] and water.[59] Neither TT-epoxide nor BB-epoxide, however, have published representative O Kα RXES spectra, so the molecular DFT code StoBe was used to simulate spectra of these two functional groups using simple representative molecules. **Figure 4** shows the comparison of the 533.2 eV and 534.6 eV O Kα RXES spectra measured from the graphene oxide paper samples against those real and simulated component spectra.

As expected, the simulated TT-epoxide molecule XES spectrum reproduced the peak structure that one sees at 533.2 eV excitation energy with surprising accuracy for all samples, despite the simplicity of the model, as Figure 4c clearly shows. The TT-epoxide simulation best models the spectrum of iGOp, but suffers when compared to GOp and rGOp largely because of peak *e*. Peak *e* at 533.2 eV emission energy lines up with the strong, narrow peak labeled H2O in Figure 2e, which suggests that peak *e* is also due to the chemisorption of water. This conclusion is strengthened by the fact that peak *e* is the most intense for GOp. A lessened peak *e* in iGOp thus suggests less water content per functional group in iGOp as compared to GOp and rGOp.

Proof that BB-epoxide is present in rGOp is seen in Figure 4d. Comparisons to O Kα RXES spectra of water and acetic acid show these two functional groups do indeed contribute to the all three spectra. However, neither water nor carboxyl can explain peak *c*. Indeed, the only reasonable explanation for this feature is given by the BB-epoxide molecule simulation, which gives an intense feature at approximately this energy. It should be noted that carbonate produces a strong spectral line at this energy as well, but carbonate has not been seen by any other author to the best of our knowledge. The TT-epoxide model also shows this feature, but its relative intensity is too small to account for peak *c* in the 534.6 eV spectra of GOp and rGOp. The functional group that is resonantly excited at either 288.2 eV on the C 1*s* edge or 534.3 eV on the O 1*s* edge is clearly BB-epoxide.

There is a clear pattern seen. In a sample with a strong TT-epoxide signal, the BB- epoxide signal is weak (iGOp), whereas in a sample with a strong contribution from BB- epoxide, the TT-epoxide component is weak (rGOp). This pattern is unrelated to the initial chemistry of the samples because iGOp was not intercalated with dodecylamine until after the sample had been created in the same manner as GOp. If initial chemistry was

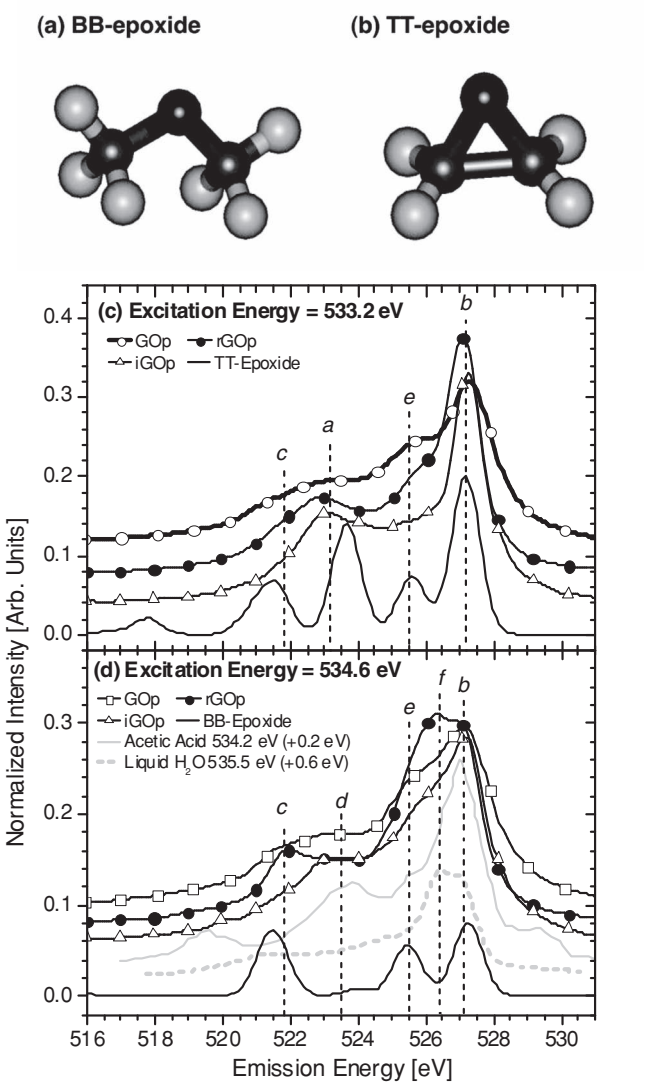

Figure 4. Component spectra that contribute to GOp, iGOp, and rGOp O Kα RXES spectra. a) Broken bond epoxide (BB-epoxide). b) Total triangle epoxide (TT-epoxide). In both panels, oxygen is colored black, carbon is dark grey, and hydrogen is light grey. Hydrogens were included to pacify the remaining carbon bonds. c) Comparison of 533.2 eV O Kα spectra from all three samples to calculated TT-epoxide. d) Comparison of 534.6 eV O Kα spectra from all three samples to calculated BB-epoxide, a digitized water spectrum from ref. [59], and a digitized acetic acid spectrum from ref. [58], The simulations in (c) and (d) were shifted such that the highest-intensity peaks in theory and experiment lined up.

the deciding factor, then iGOp and GOp should be very close. Thus, BB-epoxide is most likely the result of aging. Because epoxide is mobile at room temperature, epoxide functional groups can hop along the graphene lattice, if there is sufficient room, and align. As mentioned previously, the mechanism that promotes the unzipping of the graphene lattice is still in dispute. Li et al. calculated that epoxides would spontaneously diffuse together, line up, and fracture the lattice because alignment was energetically favorable.[36] Sun et al., however, argue that an BB-epoxide trimer is necessary first as a nucleation site, which then will draw other epoxides near to continue the process.[42] Indeed, nucleation seems vital to many of the oxidation reactions involving graphene oxide, from the initial oxidation of graphite through to thermal reduction.[60] Other authors argue that unzipping begins at the surface.[61] Nevertheless, the fact that BB-epoxide intensity grows while TT-epoxide intensity shrinks fits with the idea that TT-epoxide is being consumed over time as BB-epoxide fractures form.

The conspicuous lack of BB-epoxide in the spectra of iGOp suggests that intercalation prevents the development of BB-epoxide. Although there is some debate about how the process is initiated, we agree that diffusion of epoxides or other atomic oxygen species is necessary for linear defects to form beyond the initial nucleation sites. It would seem that intercalation, in particular with dodecylamine, inhibits the diffusion process. Ultimately, more testing with intercalation is necessary, particularly with other suitable intercalants.

3. Conclusions

We have shown that hydroxyl functional groups have a tendency to bunch together in zones of dense functionalization, whereas epoxides (at least initially) disperse move evenly. This leaves the hydroxyl functional groups electronically isolated from the non-functionalized carbon sites. The non-functionalized carbon states, on the other hand, exhibit very similar spectral characteristics when comparing GOp and rGOp. This shows that the carbon states are substantively identical before and after reduction. Although reduction does increase the sp^2/sp^3 ratio, distortions that remain on the carbon lattice prevent the emergence of true pristine graphene states.

We have also identified BB-epoxide, an allotrope of the epoxide functional group that breaks the carbon basal plane in graphene, which has been theorized to exist and observed in other carbon allotropes such as nanotubes. The spectral fingerprint of BB-epoxides is distinct and easily resolvable when observed using C 1*s* XANES and O Kα RXES spectroscopic techniques. The advent of BB-epoxide is the result of epoxides hopping along the graphene sheet over time, and is thus an aging effect. Reduction serves to make this aging effect more pronounced, whereas intercalating graphene oxide paper with dodecylamine seems to stay the process. Intercalation also tends to produce a more ordered sample, which may be a result of the intercalation process directly or perhaps represents a benefit of inhibiting formation of BB-epoxide defect lines. The overall significance is that, unless this kind of aging effect is properly mitigated during graphene oxide-based device fabrication, or at least taken into account when considering the characteristics of the device over its full lifetime, then the performance of said device may suffer deleterious degradation.

The work presented here offers important insight into how the functional groups affect the graphene basal plane as well as how one may control the form in which the functional groups present themselves, particularly epoxide. However, graphene oxide research has not yet advanced to the point where one may reliably know parameters such as the band gap and carrier mobility within a graphene oxide sample without extensive characterization and analysis. More experimentation and accurate simulation is clearly needed, and the subject of ongoing research.

4. Experimental Section

Experimental Measurements: The RXES measurements, as well as some of the XANES spectra, on the carbon and oxygen K edges were performed at Beamline 8.0.1 at the Advanced Light Source at the Lawrence Berkeley National Laboratory using the soft X-ray fluorescence (SXF) endstation.[62] Emitted radiation was measured using a Rowland circle type spectrometer with a large spherical grating and a photon-counting area detector. The total experimental resolution was 0.3 eV FWHM. The C 1*s* and O 1*s* XANES spectra were measured in total electron yield mode. The fluorescence measurements were made using a depolarized configuration, which means that the vector E of the incidence beam lies at the scattering plane, i.e., p-polarization was used. The SXF endstation was configured such that the path of the emitted photons that can be detected by the spectrometer and the incident beam are perpendicular to each other. All C 1*s* and O 1*s* XANES spectra measured at the ALS were normalized to the current generated in a highly transparent gold mesh upstream of the sample.

High-resolution XANES spectra on the C 1*s* edge were measured at the Spherical Grating Monochromator (SGM) beamline at the Canadian Light Source. The spectra were measured in both total electron yield and total fluorescence yield modes. Instead of normalizing to an upstream mesh current, however, the spectra were instead normalized to the current generated in a photodiode. This photodiode current spectrum was not taken simultaneously with the sample spectrum, but rather directly afterwards. This technique allows one to directly measure the light intensity hitting the sample as a function of energy, which allows one to correct for the problem of a carbon-contaminated mesh introducing false features into carbon spectra.

Experimental TICS Ratios: Normalization of a spectrum to its total integrated counts per second (TICS) is a very useful analytical technique as it provides a useful unit for the ordinate of a spectrum. Rather than simple counts, the ordinate is now the probability density of the energy that a photon will have per radiative decay event that involves spectator (valence) electrons. In the one-electron picture with no scattering, which holds remarkably well for non-correlated systems, the inelastic component of a spectrum is directly proportional to the occupied density of states of that system. Thus, the ordinate units can be interpreted as the probability density that an electron from a particular part of the density states will refill the core hole in a radiative decay event.

Each spectrum was normalized to its TICS value in the following way. The spectrum was first smoothed with an FFT filter. Background counts were then removed by subtraction of an appropriate parabolic background function as defined by the noise floor within the spectral measurement window but outside of the spectrum. Each spectrum was then normalized to the integrated intensity of the inelastic portion of that particular spectrum. The elastic peak contributions were isolated and removed by Gaussian peak fitting.

If one were to stop here, then one could examine the distribution of the occupied states (valence electrons) in energy space within one system, and how that distribution differs from that of another system, but any quantitative comparison between systems at a given energy level is impossible. Therefore, each spectrum taken from samples rGOp and iGOp at a given energy was renormalized to the TICS of the GOp spectrum measured while exciting at the same energy. The TICS value is directly proportional to the rate of core hole creation, so by normalizing all spectra to the same TICS value, then the TICS values all reflect the probability of a photon being produced at a given energy level for the same core hole creation rate. In short, the ability of the system to absorb incoming photons is removed from the problem, and comparing RXES spectra measured on different samples takes on a quantitative aspect as one directly measures the relative differences in density of states at a given energy.

Theoretical Calculations: The simulated XES spectra for BB-epoxide and TT-epoxide shown in Figure 4 were calculated using StoBe. This program implements Kohn-Sham DFT with both auxiliary and orbital basis sets based on the Huzinaga basis sets originally developed for Hartree-Fock calculations.[63] The orbital sets used were triple-ζ plus valence polarization (TZVP) sets containing sets of s-, p-, and d-type functions in the form (*n*s/*n*p/*n*d). The exact sets used are contained within the StoBe library and were (7111/411/1) for O and C, and (41/1*) for H. The auxiliary basis sets use blocks of s-type and spd-type functionals to model the density (*d*) and exchange correlation (ex) functionals in the form of (*exs*,*exspd*;*ds*,*dspd*), with (5,2;5,2) used for O and C, and (3,1;3,1) for H. For comparison with measurements, the simulated oxygen spectra were broadened by convolution with Gaussian functions with FWHM of 1.0 eV. **Table 3** lists the coordinates of the atoms used in each of the simulations.

Table 3. Atomic coordinates for BB-epoxide and TT-epoxide simulations. All distances are given in Å from the origin.

TT-epoxide				BB-epoxide			
Atom	X	Y	Z	Atom	X	Y	Z
O1	–6.366	0.997	0.381	O1	–5.989	1.478	0.871
C1	–7.252	2.137	0.435	C1	–6.867	2.468	0.340
C2	–7.246	1.140	1.518	C2	–6.540	0.870	2.037
H1	–6.759	3.105	0.588	H1	–7.842	2.031	0.036
H2	–6.751	1.378	2.467	H2	–6.376	2.896	–0.546
H3	–8.058	0.404	1.580	H3	–7.060	3.277	1.073
H4	–8.069	2.133	–0.297	H4	–5.810	0.133	2.395
				H5	–7.496	0.353	1.816
				H6	–6.723	1.616	2.836

Acknowledgements

All samples were made by Sasha Stankovich (at the Department of Chemistry, Northwestern University, USA). The authors acknowledge support by the Natural Sciences and Engineering Research Council of Canada (NSERC), the Canada Research Chair program and the Russian Foundation for Basic Research (Projects 11-02-00022), The Canadian Light Source is supported by NSERC, the National Research Council (NSC) Canada, the Canadian Institutes of Health Research(CIHR), the Province of Saskatchewan, Western Economic Diversification Canada, and the University of Saskatchewan. The Advanced Light Source is supported by the Director, Office of Science, Office of Basic Energy Sciences, of the U.S. Department of Energy under Contract No. DE-AC02-05CH11231.

Received: February 23, 2012
Revised: April 24, 2012
Published online: June 11, 2012

[1] K. Novoselov, A. Geim, S. Morozov, D. Jiang, Y. Zhang, S. Dubonos, I. Grigorieva, A. Firsov, *Science* **2004**, *306*, 666.
[2] K. Novoselov, A. Geim, S. Morozov, D. Jiang, M. Katsnelson, I. Grigorieva, S. Dubonos, A. Firsov, *Nature* **2005**, *438*, 197.
[3] A. Bostwick, F. Speck, T. Seyller, K. Horn, M. Polini, R. Asgari, A. H. MacDonald, E. Rotenberg, *Science* **2010**, *328*, 999.
[4] H. Wang, Q. Hao, X. Yang, L. Lu, X. Wang, *Electrochem. Commun.* **2009**, *11*, 1158.
[5] J. O. Sofo, A. S. Chaudhari, G. D. Barber, *Phys. Rev. B* **2007**, *75*, 153401.
[6] M. Z. S. Flores, P. A. S. Autreto, S. B. Legoas, D. S. Galvao, *Nanotechnology* **2009**, *20*, 465704.
[7] S. H. Lee, D. H. Lee, W. J. Lee, S. O. Kim, *Adv. Funct. Mater.* **2011**, *21*, 1338.
[8] A. K. Geim, K. S. Novoselov, *Nat. Mater.* **2007**, *6*, 183.

[9] X. Du, I. Skachko, A. Barker, E. Y. Andrei, *Nat. Nanotechnol.* **2008**, *3*, 491.
[10] S. W. Tong, Y. Wang, Y. Zheng, M.-F. Ng, K. P. Loh, *Adv. Funct. Mater.* **2011**, *21*, 4430.
[11] D. Li, M. B. Muller, S. Gilje, R. B. Kaner, G. G. Wallace, *Nat. Nanotechnol.* **2008**, *3*, 101.
[12] S. Stankovich, D. A. Dikin, R. D. Piner, K. A. Kohlhaas, A. Kleinhammes, Y. Jia, Y. Wu, S. T. Nguyen, R. S. Ruoff, *Carbon* **2007**, *45*, 1558.
[13] X. Wang, L. Zhi, K. Muellen, *Nano Lett.* **2008**, *8*, 323.
[14] J. Wu, H. A. Becerril, Z. Bao, Z. Liu, Y. Chen, P. Peumans, *Appl. Phys. Lett.* **2008**, *92*, 263302.
[15] Q. Liu, Z. Liu, X. Zhang, N. Zhang, L. Yang, S. Yin, Y. Chen, *Appl. Phys. Lett.* **2008**, *92*, 223303.
[16] Q. Liu, Z. Liu, X. Zhong, L. Yang, N. Zhang, G. Pan, S. Yin, Y. Chen, J. Wei, *Adv. Funct. Mater.* **2009**, *19*, 894.
[17] T.-F. Yeh, J.-M. Syu, C. Cheng, T.-H. Chang, H. Teng, *Adv. Funct. Mater.* **2010**, *20*, 2255.
[18] J. T. Robinson, F. K. Perkins, E. S. Snow, Z. Wei, P. E. Sheehan, *Nano Lett.* **2008**, *8*, 3137.
[19] R. A. Nistor, D. M. Newns, G. J. Martyna, *ACS Nano* **2011**, *5*, 3096.
[20] K.-H. Liao, A. Mittal, S. Bose, C. Leighton, K. A. Mkhoyan, C. W. Macosko, *ACS Nano* **2011**, *5*, 1253.
[21] P. Avouris, Z. Chen, V. Perebeinos, *Nat. Nanotechnol.* **2007**, *2*, 605.
[22] D. W. Boukhvalov, M. I. Katsnelson, *J. Am. Chem. Soc.* **2008**, *130*, 10697.
[23] J. T. Paci, T. Belytschko, G. C. Schatz, *J. Phys. Chem. C* **2007**, *111*, 18099.
[24] Z. Xu, K. Xue, *Nanotechnology* **2010**, *21*, 045704.
[25] J.-A. Yan, L. Xian, M. Y. Chou, *Phys. Rev. Lett.* **2009**, *103*, 086802.
[26] R. J. W. E. Lahaye, H. K. Jeong, C. Y. Park, Y. H. Lee, *Phys. Rev. B* **2009**, *79*, 125435.
[27] A. Lerf, H. He, M. Forster, J. Klinowski, *J. Phys. Chem. B* **1998**, *102*, 4477.
[28] H. He, J. Klinowski, M. Forster, A. Lerf, *Chem. Phys. Lett.* **1998**, *287*, 53.
[29] J. Chattopadhyay, A. Mukherjee, C. E. Hamilton, J. Kang, S. Chakraborty, W. Guo, K. F. Kelly, A. R. Barron, W. E. Billups, *J. Am. Chem. Soc.* **2008**, *130*, 5414.
[30] K. A. Mkhoyan, A. W. Contryman, J. Silcox, D. A. Stewart, G. Eda, C. Mattevi, S. Miller, M. Chhowalla, *Nano Lett.* **2009**, *9*, 1058.
[31] D. Pacile, M. Papagno, A. F. Rodriguez, M. Grioni, L. Papagno, *Phys. Rev. Lett.* **2008**, *101*, 066806.
[32] M. Papagno, A. F. Rodriguez, C. O. Girit, J. C. Meyer, A. Zettl, D. Pacile, *Chem. Phys. Lett.* **2009**, *475*, 269.
[33] V. Lee, L. Whittaker, C. Jaye, K. M. Baroudi, D. A. Fischer, S. Banerjee, *Chem. Mater.* **2009**, *21*, 3905.
[34] V. Lee, C. Park, C. Jaye, D. A. Fischer, Q. Yu, W. Wu, Z. Liu, S.-S. Pei, C. Smith, P. Lysaght, S. Banerjee, *J. Phys. Chem. Lett.* **2010**, *1*, 1247.
[35] H. K. Jeong, H. J. Noh, J. Y. Kim, M. H. Jin, C. Y. Park, Y. H. Lee, *EPL* **2008**, *82*, 67004.
[36] J. Li, K. Kudin, M. McAllister, R. Prud'homme, I. Aksay, R. Car, *Phys. Rev. Lett.* **2006**, *96*, 176101.
[37] D. B. Shinde, J. Debgupta, A. Kushwaha, M. Aslam, V. K. Pillai, *J. Am. Chem. Soc.* **2011**, *133*, 4168.
[38] D. A. Dikin, S. Stankovich, E. J. Zimney, R. D. Piner, G. H. B. Dommett, G. Evmenenko, S. T. Nguyen, R. S. Ruoff, *Nature* **2007**, *448*, 457.
[39] S. Stankovich, D. A. Dikin, O. C. Compton, G. H. B. Dommett, R. S. Ruoff, S. T. Nguyen, *Chem. Mater.* **2010**, *22*, 4153.
[40] I. Christl, R. Kretzschmar, *Environ. Sci. Technol.* **2007**, *41*, 1915.
[41] W. Zhang, V. Carravetta, Z. Li, Y. Luo, J. Yang, *J. Chem. Phys.* **2009**, *131*, 244505.
[42] T. Sun, S. Fabris, *Nano Lett.* **2012**, *12*, 17.
[43] P. Ajayan, B. Yakobson, *Nature* **2006**, *441*, 818.
[44] P. Johari, V. B. Shenoy, *ACS Nano* **2011**, *5*, 7640.
[45] W. Cai, R. D. Piner, F. J. Stadermann, S. Park, M. A. Shaibat, Y. Ishii, D. Yang, A. Velamakanni, S. J. An, M. Stoller, J. An, D. Chen, R. S. Ruoff, *Science* **2008**, *321*, 1815.
[46] A. Bagri, C. Mattevi, M. Acik, Y. J. Chabal, M. Chhowalla, V. B. Shenoy, *Nat. Chem.* **2010**, *2*, 581.
[47] C. Gomez-Navarro, J. C. Meyer, R. S. Sundaram, A. Chuvilin, S. Kurasch, M. Burghard, K. Kern, U. Kaiser, *Nano Lett.* **2010**, *10*, 1144.
[48] D. W. Lee, L. De Los Santos V, J. W. Seo, L. L. Felix, A. Bustamante D, J. M. Cole, C. H. W. Barnes, *J. Phys. Chem. B* **2010**, *114*, 5723.
[49] H.-K. Jeong, L. Colakerol, M. H. Jin, P.-A. Glans, K. E. Smith, Y. H. Lee, *Chem. Phys. Lett.* **2008**, *460*, 499.
[50] H.-K. Jeong, Y. P. Lee, R. J. W. E. Lahaye, M.-H. Park, K. H. An, I. J. Kim, C.-W. Yang, C. Y. Park, R. S. Ruoff, Y. H. Lee, *J. Am. Chem. Soc.* **2008**, *130*, 1362.
[51] S. Biniak, G. Szymanski, J. Siedlewski, A. Swiatkowski, *Carbon* **1997**, *35*, 1799.
[52] V. Datsyuk, M. Kalyva, K. Papagelis, J. Parthenios, D. Tasis, A. Siokou, I. Kallitsis, C. Galiotis, *Carbon* **2008**, *46*, 833.
[53] D. R. Dreyer, S. Park, C. W. Bielawski, R. S. Ruoff, *Chem. Soc. Rev.* **2010**, *39*, 228.
[54] C. Hontoria-Lucas, A. Lopez-Peinado, J. Lopez-Gonzalez, M. Rojas-Cervantes, R. Martin-Aranda, *Carbon* **1995**, *33*, 1585.
[55] C. Mattevi, G. Eda, S. Agnoli, S. Miller, K. A. Mkhoyan, O. Celik, D. Mostrogiovanni, G. Granozzi, E. Garfunkel, M. Chhowalla, *Adv. Funct. Mater.* **2009**, *19*, 2577.
[56] C.-Y. Su, Y. Xu, W. Zhang, J. Zhao, X. Tang, C.-H. Tsai, L.-J. Li, *Chem. Mater.* **2009**, *21*, 5674.
[57] Z.-S. Wu, W. Ren, L. Gao, B. Liu, C. Jiang, H.-M. Cheng, *Carbon* **2009**, *47*, 493.
[58] T. Tokushima, Y. Horikawa, Y. Harada, O. Takahashi, A. Hiraya, S. Shin, *Phys. Chem. Chem. Phys.* **2009**, *11*, 1679.
[59] T. Tokushima, Y. Harada, O. Takahashi, Y. Senba, H. Ohashi, L. G. M. Pettersson, A. Nilsson, S. Shin, *Chem. Phys. Lett.* **2008**, *460*, 387.
[60] T. Sun, S. Fabris, S. Baroni, *J. Phys. Chem. C* **2011**, *115*, 4730.
[61] Z. Li, W. Zhang, Y. Luo, J. Yang, J. G. Hou, *J. Am. Chem. Soc.* **2009**, *131*, 6320.
[62] J. J. Jia, T. A. Callcott, J. Yurkas, A. W. Ellis, F. J. Himpsel, M. G. Samant, J. Stohr, D. L. Ederer, J. A. Carlisle, E. A. Hudson, L. J. Terminello, D. K. Shuh, R. C. C. Perera, *Rev. Sci. Instrum.* **1995**, *66*, 1394.
[63] K. Hermann, L. G. M. Pettersson, *Documentation for StoBe 2011* (www.fhi-berlin.mpg.bde/KHsoftware/StoBe/StoBeMAN.html), 3rd ed., **2011.**